JOURNAL OF GEOPHYSICAL RESEARCH, VOL. 104, NO. B1, PAGES 617–628, JANUARY 10, 1999

# Single-domain critical sizes for coercivity and remanence

Andrew J. Newell[1] and Ronald T. Merrill
Geophysics Program, University of Washington, Seattle, Washington

**Abstract.** It is usually assumed that magnetic parameters such as coercivity and saturation remanence are single-domain (SD) over the same size range. In reality, there is a different SD size range for each parameter. We define critical sizes $L_{\mathrm{SD}}^{\mathrm{coerc}}$ for coercivity and $L_{\mathrm{SD}}^{\mathrm{rem}}$ for remanence. In general, $L_{\mathrm{SD}}^{\mathrm{coerc}} \leq L_{\mathrm{SD}}^{\mathrm{rem}}$. Up to $L = L_{\mathrm{SD}}^{\mathrm{rem}}$, the saturation remanent state is single-domain. If a sufficiently large reverse field is applied, a conventional SD state would reverse by uniform rotation. However, the mode of reversal is nonuniform if the grain size is between $L_{\mathrm{SD}}^{\mathrm{coerc}}$ and $L_{\mathrm{SD}}^{\mathrm{rem}}$, so in this size range the SD state is less stable. To calculate the critical sizes, we use rigorous nucleation theory and obtain analytical expressions. The analytical form allows us to explore the effect of grain shape, stress, crystallographic orientation and titanium content in titanomagnetites. We adapt the theory to cubic anisotropy with $K_1 < 0$, which allows us to apply the expressions to titanomagnetites. We find that the size range for SD coercivity is always small. The size range for SD remanence can vary enormously depending on the anisotropy. If the easy axes are oriented favorably, the SD state can occur in large $x = 0.6$ titanomagnetite grains. Ensembles of magnetite grains with aspect ratios greater than 5 have SD-like remanence but low coercivity. However, most synthetic magnetite grains are nearly equant, and the predicted size range for SD remanence is small to nonexistent. This, rather than grain interactions, may be the reason they have properties such as saturation remanence that do not agree well with standard SD theory.

## 1. Introduction

Of the factors that determine the magnetic properties of rocks, grain size is exceeded in importance only by chemical composition. Hysteresis parameters like the coercivity $H_c$ and the remanence $M_{rs}$ increase rapidly with grain size and then decrease rapidly. The changes in these parameters correspond to changes in the microscopic behavior of the magnetization. Rock magnetists have traditionally divided grain sizes into four ranges on the basis of the pattern of magnetization in zero field (the remanent state). Superparamagnetic (SPM) grains respond reversibly to magnetic fields and have zero remanence. In single-domain (SD) grains, the magnetization is uniform in zero field. Pseudo-single-domain (PSD) and multidomain (MD) grains have a nonuniform remanent state.

The single-domain size range is of particular interest to Earth scientists for many reasons [*Dunlop and Özdemir,* 1997]. For example, environmental magnetists use parameters such as $H_c$ and $M_{rs}$ to infer the size of magnetic grains [*Thompson and Oldfield,* 1986; *Opdyke and Channell,* 1996]. Paleomagnetists consider single-domain grains to be important in part because they carry a remanence that tends to be stable over geological timescales. Estimates of the SD size range have also been used to support evolutionary arguments for navigation using ferromagnetic particles [*Kirschvink and Lowenstam,* 1979; *Ricci and Kirschvink,* 1992].

Rock magnetists often assume that there is a single critical size $L_0$ separating uniform from nonuniform remanence, and that all the magnetic properties change suddenly across $L_0$. By this assumption, parameters such as $H_c$ and $M_{rs}$ would have the same size dependence. In reality, they often do not. For example, *Levi and Merrill* [1978] observed needles of magnetite with single-domain remanence but a comparatively low coercivity. Nor are the uniform and nonuniform remanent states clearly separated by size, because the remanent state depends on the history of the grain. Grains can have a SD saturation remanent state and then develop domain walls in reverse fields [*Halgedahl and Fuller,* 1980, 1983; *Boyd et al.,* 1984].

Instead of a general SD critical size, we need to calculate critical sizes for particular magnetic properties. In this paper we define critical sizes for coercivity and remanence and calculate them using a rigorous stability

[1]Now at Scripps Institution of Oceanography, La Jolla, California.



Paper number 1998JB900039.
0148-0227/99/1998JB900039$09.00

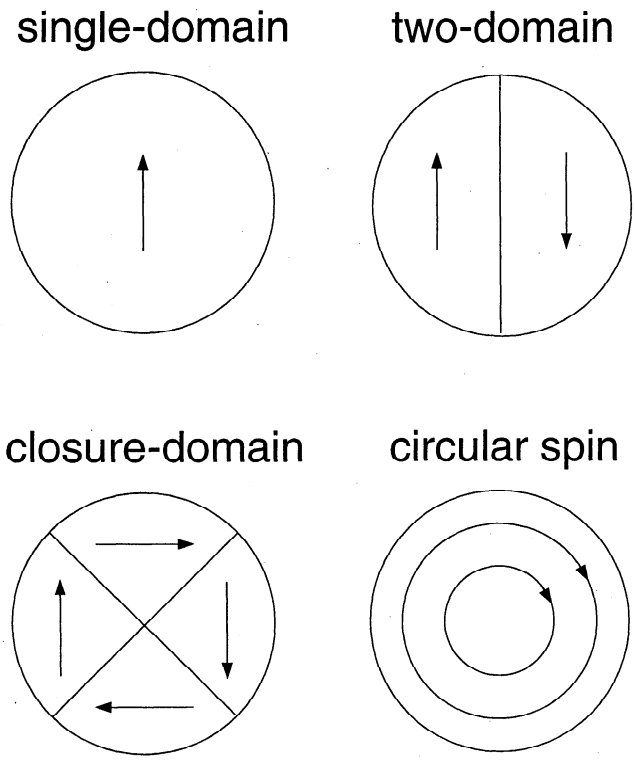


**Figure 1.** Four candidate domain states. The arrows are the magnetization, and the straight lines are domain walls.

theory (nucleation theory). In section 1.1, we describe previous attempts to calculate the critical size $L_0$, and in section 1.2 we introduce nucleation theory.

### 1.1. Lowest-Energy State

In early attempts at calculating the SD size range, theorists guessed the nonuniform state, or multidomain (MD) state, and estimated its energy as a function of grain size. The critical size $L_0$, which we will call the SD energy critical size, was defined as the size at which the energy of the MD state was equal to the energy of the SD state. Some examples of proposed states are shown in Figure 1. The two-domain and closure-domain states [*Kittel*, 1946, 1949] have uniformly magnetized domains separated by thin domain walls. The Kittel models were applied to rock magnetism by *Stacey* [1963].

In the energy calculations for the two-domain state, the internal structure of the domain wall was derived for an infinite body [*Landau and Lifshitz*, 1935]. As a result, its predicted thickness was independent of grain size. *Néel* [1947] pointed out that when the magnetocrystalline anisotropy was small (as in iron or magnetite), the predicted critical size $L_0$ was less than the thickness of the domain wall. For such materials, he proposed a state with a circular magnetization pattern (Figure 1) and used it to calculate the critical size for a sphere of low-anisotropy material. *Morrish and Yu* [1955] generalized his calculation to ellipsoids of rotation, and their results were applied to rock magnetism by *Nagata* [1961] and *Evans and McElhinny* [1969].

The above calculations were for ellipsoids. *Butler and Banerjee* [1975] argued that the faceted crystals commonly found in rocks were better represented by cuboids (rectangular parallelepipeds). In calculating the energy of a two-domain state in a cuboid, they allowed the width of the domain wall to vary and included the magnetostatic energy of the wall in the calculation. As a result, the wall width depended on the grain size and occupied about half of the grain at the critical size.

While the two-domain and circular spin models are still widely quoted in textbooks on paleomagnetism and rock magnetism [e.g., *Dunlop and Özdemir*, 1997], they are only models, not rigorous solutions for the magnetization. As the above history suggests, the accuracy of such a model depends on the ingenuity of the theorist who tries to guess the structure of the lowest-energy state. Since the energy calculations involve approximations of unknown accuracy, there is no way of telling whether any of them is close to the real solution.

In micromagnetic theory [*Brown*, 1963], one tries to solve for the magnetization without placing constraints on the structure. The energy terms are the same as in domain theories, but the magnetization is allowed to vary continuously. By minimizing the energy using variational calculus, differential equations for the magnetization are obtained. These equations are difficult to solve, so most solutions are numerical. In solutions for magnetite [*Newell et al.*, 1993; *Williams and Dunlop*, 1989; *Fabian et al.*, 1996], the lowest-energy nonuniform states are called curling, or vortex, states. These states are more like the circular spin state than the two-domain state.

While a numerical micromagnetic solution is less constrained than a domain model, it still uses numerical approximations, and the uncertainties in the approximations have not been quantified. The solution sometimes changes dramatically when the grid size is refined.

### 1.2. Multiple States and Stability

Before the 1980s, most researchers implicitly assumed that a grain must always be in its lowest-energy magnetic state, which in domain models was SD for $L < L_0$ and MD for $L > L_0$. However, *Halgedahl and Fuller* [1980, 1983] observed different numbers of domains in the same grain. To explain this observation, *Moon and Merrill* [1984] used micromagnetic theory to show that more than one state could occur in a grain depending on the grain's history.

Since there are multiple remanent states, we need to know when transitions occur between states. For there to be a transition, a state must become unstable. Some rock magnetists [*Moon and Merrill*, 1984; *Enkin and Dunlop*, 1987; *Moskowitz and Halgedahl*, 1987; *Newell et al.*, 1990] have tried to calculate the size range for stability of the SD state, but in each calculation some constraint was imposed, and it was not clear whether the instability was physical or numerical.

The purpose of nucleation theory is to derive rigorous conditions for the stability of a state $\mathbf{M}(\mathbf{r})$. This is done

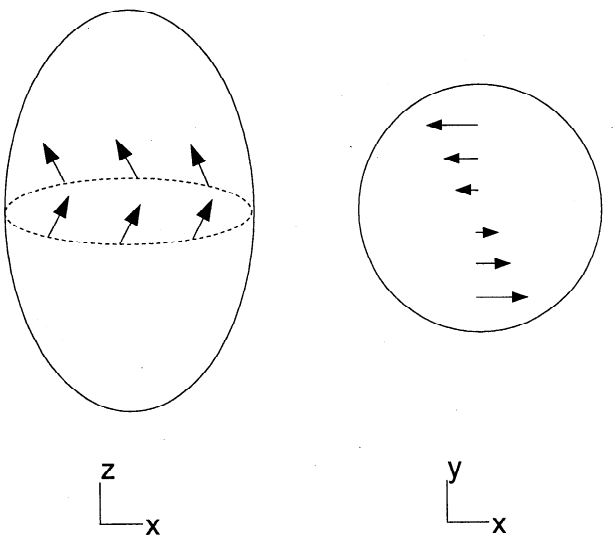


**Figure 2.** A sketch of the curling mode perturbation added to a uniform magnetization in the $z$ direction. For visibility, the perturbation is greatly exaggerated; in the nucleation calculations, the change in $m_z$ is negligible.

by adding a perturbation $\Delta\mathbf{M} = \epsilon M_s \mathbf{u}$, where $\epsilon \ll 1$ and $\mathbf{u}$ is a function of position $\mathbf{r}$. If the perturbation lowers the energy, the initial state is unstable. If the initial state is the SD state, the perturbation that causes the instability is called a nucleation mode and the field at which it occurs is the nucleation field.

The nucleation field has been calculated analytically for prolate and oblate spheroids (ellipsoids of rotation) [*Aharoni,* 1959, 1966]. Spheroidal grains have the advantage that the demagnetizing field of the initial state (usually the most difficult part of the calculation) is uniform and the micromagnetic equations can be linearized. One nucleation mode is uniform rotation. Another, the curling mode (Figure 2), is one of a class of modes that have no radial component. In cylindrical coordinates (with the initial magnetization in the $z$ direction), the curling modes have the form

$$u_\phi = u_\phi(\rho, z) \qquad u_\rho = u_z = 0. \tag{1}$$

*Aharoni* [1966] showed that uniform rotation and the lowest order curling mode (which we will just call the curling mode hereafter) are the only possible nucleation modes in oblate spheroids. Both modes also occur in prolate spheroids. It was long thought that there might be a third nucleation mode in prolate spheroids called buckling; this mode is sometimes a solution for infinite cylinders [*Aharoni and Shtrikman,* 1958]. Recently, *Aharoni* [1997] showed that the buckling mode does not occur in spheroids with aspect ratios below 500:1. Thus for all practical purposes, the only nucleation modes in spheroids are uniform rotation and curling.

The existing derivations for the nucleation field are for uniaxial or cubic magnetocrystalline anisotropy with $K_1 > 0$. A highly symmetric geometry is assumed where a magnetocrystalline easy axis is aligned with the rotational axis of the spheroid. We will show that if the orientation of the easy axis is changed, the nucleation field can decrease considerably. In addition, we will calculate the nucleation field for cubic anisotropy with $K_1 < 0$ and apply the results to titanomagnetites.

We will also attempt to make nucleation theory more useful to rock magnetists by clarifying its relevance to remanent states and hysteresis. Experimentalists and theorists use the word "nucleation" in different ways. For the experimentalists, it is the first appearance of a domain wall. For the theorist, it is the first deviation from the SD state. These events do not coincide. We use the theoretical definition in this paper and show that it always precedes domain wall formation.

Our main application of nucleation theory will be to calculate two important critical sizes: $L_{\mathrm{SD}}^{\mathrm{coerc}}$, the upper limit for nucleation by uniform rotation, and $L_{\mathrm{SD}}^{\mathrm{rem}}$, the upper limit for SD remanence. These critical sizes have been calculated before using nucleation theory [*Brown,* 1963; *Aharoni and Shtrikman,* 1958], but their differences were not emphasized. They were not even distinguished by name, it being implicitly assumed that they were nearly equal to each other and to $L_0$. We will show that $L_{\mathrm{SD}}^{\mathrm{coerc}}$ and $L_{\mathrm{SD}}^{\mathrm{rem}}$ can be very different from each other, and we will discuss the consequences for hysteresis properties.

## 2. Critical Size Calculations

In this section, we begin by calculating the nucleation field, with the effects of crystallographic orientation and stress included. We then derive expressions for the critical sizes $L_{\mathrm{SD}}^{\mathrm{coerc}}$ and $L_{\mathrm{SD}}^{\mathrm{rem}}$. Finally, we use these expressions to calculate critical sizes for some titanomagnetites and compare them with domain observations.

### 2.1. Nucleation Field Calculations

In a ferromagnet, the magnetization $\mathbf{M}$ has variable direction but fixed magnitude $M_s$, where $M_s$ is called the saturation magnetization. It can therefore be represented by a unit vector

$$\hat{\mathbf{m}} = \mathbf{M}/M_s = m_x\hat{\mathbf{i}} + m_y\hat{\mathbf{j}} + m_z\hat{\mathbf{k}}, \tag{2}$$

where $m_x^2 + m_y^2 + m_z^2 = 1$.

For a given temperature and external field $\mathbf{H}$, the free energy $G$ is a minimum in equilibrium [*Brown,* 1963]. This energy is an integral over the volume $V$ of the ferromagnet:

$$G = \int_V \Big\{ A\left[(\nabla m_x)^2 + (\nabla m_y)^2 + (\nabla m_z)^2\right] - \frac{\mu_0}{2}\mathbf{M}\cdot\mathbf{H_d} - \mu_0\mathbf{M}\cdot\mathbf{H} + g_a + g_\lambda \Big\}\, d^3\mathbf{r}, \tag{3}$$

where $A$ is the exchange constant, $\mathbf{H_d}$ is the demagnetizing field, $\mathbf{H}$ is the applied field, $g_a$ is the magnetocrystalline energy density, and $g_\lambda$ is the inverse magnetostriction energy density.

In the following calculations, we assume the grain is a spheroid (ellipsoid of rotation). The axis of rotational symmetry of the spheroid, the external magnetic field

and a magnetocrystalline easy axis are all aligned with the $z$ axis. Because of the rotational symmetry, the magnetic moment must also be in the $z$ direction. The dimensions of the spheroid are the major axis $Z$ and the minor axis $X$. Previous authors have used various definitions for grain size, including the major or minor axis. We define the size $L$ as the cube root of the volume. This definition is equally applicable to grains of any shape, and it separates the effects of volume and shape.

The initial state for the nucleation calculations is one of uniform magnetization ($m_x = m_y = 0, m_z = 1$). Since $\hat{\mathbf{m}}$ has a fixed magnitude and can only rotate, any perturbation is perpendicular to $\hat{\mathbf{m}}$ and has the form $\Delta m_x = \epsilon u_x, \Delta m_y = \epsilon u_y$, and $\Delta m_z = 0$. We add such a perturbation to $\hat{\mathbf{m}}$ and expand the free energy to second order in $\epsilon$.

To illustrate the procedure, we will calculate the nucleation field for uniform rotation. If the only source of anisotropy is magnetostatic (from grain shape), the energy is $G = gV$, where

$$g = \frac{1}{2}\mu_0 M_s^2 (N_x m_x^2 + N_y m_y^2 + N_z m_z^2) - \mu_0 M_s H m_z.$$

In this expression, $N_x, N_y$, and $N_z$ are the demagnetizing factors corresponding to the $x, y$, and $z$ axes. For the magnetization to be along the $z$ axis in zero field, we require $N_x \geq N_y \geq N_z$. With the perturbation added, the magnetization is $m_x = \epsilon u_x, m_y = \epsilon u_y$, and $m_z = \left(1 - \epsilon^2 u_x^2 - \epsilon^2 u_y^2\right)^{1/2}$. Expanding the energy in $\epsilon$ and ignoring constants,

$$g \approx \left[\frac{1}{2}\mu_0 M_s^2 (N_x - N_z) + \frac{1}{2}\mu_0 M_s H\right] \epsilon^2 (u_x^2 + u_y^2)$$

If, for some choice of $u_x$ and $u_y$, $\partial G/\partial\epsilon = \partial^2 G/\partial\epsilon^2 = 0$, the initial state is unstable. From the above equation, this occurs when $H = -(N_x - N_z) M_s$.

If there are other sources of anisotropy, their effective fields are simply added to the nucleation field. For example, if a uniaxial magnetocrystalline anisotropy is included, the nucleation field is

$$H_n^{\text{unif}} = -(N_x - N_z) M_s - \frac{2K_1}{\mu_0 M_s}. \tag{4}$$

The above stability calculations are for uniform rotation. More generally, $u_x$ and $u_y$ can be functions of position. For the general case, the following equations are obtained using variational calculus [*Aharoni*, 1996]:

$$\left[A\nabla^2 - \kappa - \frac{1}{2}\mu_0 M_s H_n'\right] u_x + \frac{1}{2}\mu_0 M_s H_x' = 0 \tag{5}$$

$$\left[A\nabla^2 - \kappa - \frac{1}{2}\mu_0 M_s H_n'\right] u_y + \frac{1}{2}\mu_0 M_s H_y' = 0 \tag{6}$$

with the boundary conditions

$$\frac{\partial u_x}{\partial n} = \frac{\partial u_y}{\partial n} = 0 \tag{7}$$

at the surface of the grain. In the above equations, $n$ is the component in the direction of the outward surface normal, $H_n' = H_n - N_z M_s$ and $\mathbf{H}' = (H_x', H_y', H_z')$ is the demagnetizing field due to the perturbation. The coefficient $\kappa$ is the coefficient of $\epsilon^2 \left(u_x^2 + u_y^2\right)$ in the expansion of the magnetocrystalline energy (see section 2.1.1). If we derive the nucleation field for $\kappa = 0$, then we can include the effect of nonzero $\kappa$ by adding a term $-2\kappa/\mu_0 M_s$ to the nucleation field.

Equations (5)-(7) have an infinite set of solutions, each with their own nucleation field $H_n$. However, only the largest such field has any physical meaning because below this field the SD state is already unstable. The solutions that are physically meaningful are uniform rotation and curling.

The nucleation field for the curling mode is [*Aharoni*, 1959, 1966]

$$H_n^{\text{curl}} = N_z M_s - k M_s \left(\frac{q^{1/3} L_{ex}}{L}\right)^2 - \frac{2\kappa}{\mu_0 M_s} \tag{8}$$

where $q = Z/X$ is the aspect ratio. The exchange length, $L_{ex} = \left(A/\mu_0 M_s^2\right)^{1/2}$, where $A$ is the exchange constant, is a scale length over which the magnetization can vary. The factor $q^{1/3}$ is not in the original equations by Aharoni because he defined the size as the minor axis $X = Lq^{-1/3}$.

The dimensionless parameter $k$ can be expressed as the first zero of the derivative of a spheroidal harmonic. Because of differences in units, normalization, and definition of grain size, the values of $k$ given by *Aharoni* [1959, 1966] must be multiplied by $2\pi(4\pi/3)^{2/3} = 16.3$. This parameter does not vary much with aspect ratio; it is 23.3 for an infinite plate ($q = 0$) and decreases monotonically through 22.5 for a sphere ($q = 1$) to 17.6 for an infinite cylinder ($q = \infty$).

**2.1.1. Magnetocrystalline anisotropy.** In deriving the magnetocrystalline anisotropy parameter $\kappa$ in (8), we must keep in mind that the energy density $g_a$ is expressed in terms of the crystallographic coordinates. We will denote the direction cosines of the magnetization along the [100], [010], and [001] axes by $\tilde{m}_x, \tilde{m}_y$, and $\tilde{m}_z$.

For uniaxial anisotropy,

$$g_a = K_1 \left(1 - \tilde{m}_z^2\right).$$

If the [001] axis is in the $z$ direction, then $\tilde{m}_z = m_z$, so

$$g_a = K_1 \left(1 - m_z^2\right) = K_1 \epsilon^2 \left(u_x^2 + u_y^2\right),$$

and therefore $\kappa = K_1$.

For cubic anisotropy, the energy density is

$$g_a = K_1 (\tilde{m}_x^2 \tilde{m}_y^2 + \tilde{m}_y^2 \tilde{m}_z^2 + \tilde{m}_z^2 \tilde{m}_x^2).$$

If a $\langle 001 \rangle$ axis is in the $z$ direction, then we can choose the coordinates so $m_x = \tilde{m}_x$, $m_y = \tilde{m}_y$ and $m_z = \tilde{m}_z$. To second order,

$$g_a \approx K_1 \epsilon^2 \left(u_x^2 + u_y^2\right),$$

so $\kappa = K_1$ again. If a ⟨111⟩ axis is in the $z$ direction, we choose the coordinates so $m_x, m_y$, and $m_z$ are the direction cosines of the magnetization in the $[1\bar{1}0]$, $[11\bar{2}]$, and [111] directions. Then

$$\begin{pmatrix} \tilde{m}_x \\ \tilde{m}_y \\ \tilde{m}_z \end{pmatrix} = \begin{pmatrix} 1/\sqrt{2} & 1/\sqrt{6} & 1/\sqrt{3} \\ -1/\sqrt{2} & 1/\sqrt{6} & 1/\sqrt{3} \\ 0 & -2/\sqrt{6} & 1/\sqrt{3} \end{pmatrix} \begin{pmatrix} m_x \\ m_y \\ m_z \end{pmatrix} \tag{9}$$

The second order expansion of the energy is then

$$g_a \approx -(2/3)K_1\epsilon^2 \left(u_x^2 + u_y^2\right),$$

so $\kappa = -(2/3)K_1$.

For cubic anisotropy with $K_1 > 0$, the easy axes are the ⟨001⟩ axes, and the hard axes are the ⟨111⟩ axes. The above equations are correct even if the specified axis is a hard axis, but we must be careful when we calculate the critical sizes (section 2.2).

In the above calculations, the coefficients for $u_x^2$ and $u_y^2$ in the expansion of the energy are equal. This is implicitly assumed in the derivation of equations (5)-(6). If they are not equal, we cannot simply add an effective field for magnetocrystalline anisotropy to the nucleation field. The expressions we derive in this paper apply to titanomagnetites but not to hematite or pyrrhotite, which have sixfold easy axes within a basal plane. In such materials, a rotation out of the basal plane is more difficult than a rotation within the plane. The nucleation modes in hematite and pyrrhotite may be more like domain wall motion.

**2.1.2. Magnetostriction.** If the effect of magnetostriction is included, the nucleation field for uniform rotation is obtained simply by replacing the "zero-strain" constant $K_1$ by the "zero-stress" constant $K_1'$. Fortunately, most methods for measuring anisotropy actually measure $K_1'$ [*Ye et al.*, 1994]. No one has obtained an explicit expression for the nucleation field that includes the effect of magnetostriction. However, if we replace $K_1$ with $K_1'$, we will obtain a lower bound for the actual nucleation field [*Brown*, 1963], and the error is probably small.

**2.1.3. Stress.** If a uniaxial stress $\sigma$ is applied in the direction $(\gamma_x, \gamma_y, \gamma_z)$, where $\gamma_x^2 + \gamma_y^2 + \gamma_z^2 = 1$, the inverse magnetostriction energy density is [*Chikazumi*, 1964]

$$\begin{aligned} g_\lambda = & -3\lambda_{111}\sigma \left(m_x m_y \gamma_x \gamma_y + m_y m_z \gamma_y \gamma_z + m_z m_x \gamma_z \gamma_x\right) \\ & -\frac{3}{2}\lambda_{100}\sigma \left(m_x^2\gamma_x^2 + m_y^2\gamma_y^2 + m_z^2\gamma_z^2\right). \end{aligned}$$

Thus for a stress in the [001] direction, the energy is

$$g_\lambda = -\frac{3}{2}\lambda_{100}\sigma m_z^2 \approx \frac{3}{2}\lambda_{100}\sigma\epsilon^2 \left(u_x^2 + u_y^2\right).$$

If the stress is in the [111] direction, $\sigma_{ij} = \sigma/3$ for all $i$ and $j$. Defining $m_x, m_y$, and $m_z$ as in (9),

$$g_\lambda \approx \frac{3}{2}\lambda_{111}\sigma\epsilon^2 \left(u_x^2 + u_y^2\right) + \text{const.}$$

**2.1.4. Combining the effects.** With the magnetocrystalline and magnetoelastic effects added, the nucleation field for uniform rotation is

$$H_n^{\text{unif}} = (N_z - N_x)\, M_s - H_K - H_\lambda, \tag{10}$$

and the nucleation field for curling is

$$H_n^{\text{curl}} = N_z M_s - k M_s \left(\frac{q^{1/3} L_{ex}}{L}\right)^2 - H_K - H_\lambda, \tag{11}$$

where

$$H_K = \begin{cases} 2K_1'/\mu_0 M_s, & \langle 001\rangle \text{ axis in } z \text{ direction} \\ -4K_1'/3\mu_0 M_s, & \langle 111\rangle \text{ axis in } z \text{ direction} \end{cases} \tag{12}$$

$$H_\lambda = \begin{cases} 3\lambda_{100}\sigma/\mu_0 M_s, & \text{stress in } \langle 001\rangle \text{ direction} \\ 3\lambda_{111}\sigma/\mu_0 M_s, & \text{stress in } \langle 111\rangle \text{ direction.} \end{cases} \tag{13}$$

Again, $q$ is the aspect ratio, and $L_{ex} = \left(A/\mu_0 M_s^2\right)^{1/2}$.

The above equations can be applied to both prolate and oblate spheroids. For a prolate ($q > 1$) spheroid [*Chikazumi*, 1964],

$$N_z = q(q^2-1)^{-3/2} \cosh^{-1} q - (q^2-1)^{-1}. \tag{14}$$

For an oblate ($q < 1$) spheroid,

$$N_z = -q(1-q^2)^{-3/2} \cos^{-1} q + (1-q^2)^{-1}. \tag{15}$$

In both cases, $N_x = (1 - N_z)/2$.

## 2.2. Expressions for the Critical Sizes

If $H_n^{\text{curl}} < H_n^{\text{unif}}$, the magnetization is uniform in any uniform applied field and it can change only by uniform rotation. We define the SD coercivity critical size $L_{\text{SD}}^{\text{coerc}}$ as the size at which $H_n^{\text{curl}} = H_n^{\text{unif}}$. Applying (10) and (11),

$$L_{\text{SD}}^{\text{coerc}} = q^{1/3} L_{ex} \left(\frac{k}{N_x}\right)^{1/2}. \tag{16}$$

The SD remanence critical size is the size at which SD remanence becomes unstable, or $H_n^{\text{curl}} = 0$:

$$L_{\text{SD}}^{\text{rem}} = q^{1/3} L_{ex} \left(\frac{k}{N_z}\right)^{1/2} \left(1 - \frac{H_K + H_\lambda}{M_s N_z}\right)^{-1/2}. \tag{17}$$

If we apply (17) to an oblate spheroid, we must make sure that $H_n^{\text{unif}} > 0$, so there is a stable remanent state with moment along the rotational axis. Otherwise, the expression for $L_{\text{SD}}^{\text{rem}}$ is meaningless.

Strictly speaking, the parameter $k$ depends on the aspect ratio, but the dependence is weak, and $k$ appears inside a square root in the above expressions. Using $k = 20$ for all aspect ratios introduces an error of at most 7%.

We also need a lower bound for the SD size range. We use the theory of *Néel* [1949] to calculate the critical size $L_{\text{SPM}}$ for the transition from superparamagnetism to single-domain hysteresis. For a given temperature $T$, the critical volume $V_s$ at the SPM-SD transition satisfies the blocking criterion

$$V_s = \frac{k_B T}{\Delta g} \ln\left(\frac{\tau_s}{\tau_0}\right), \tag{18}$$

where $k_B$ is the Boltzmann constant, $\tau_s$ is the time scale of interest, $\tau_0$ is a characteristic relaxation time, and $\Delta g V$ is the energy barrier separating minima. The parameter $\tau_0$ is different for uniaxial and cubic anisotropy but probably not different enough to affect the critical sizes significantly [*Aharoni*, 1996]. The critical size $L_{\rm SPM}$ is defined as $V_s^{1/3}$.

For $K_1' < 0$ and the [111] easy axis aligned with the rotational axis of the spheroid, the energy barrier is the difference in energy between the [111] direction and the [1$\bar{1}$0] direction. The latter is the saddle point for magnetocrystalline anisotropy and the hard direction for magnetostatic energy. We add the energy terms to obtain

$$\Delta g = \frac{1}{2}\mu_0 M_s^2 (N_x - N_z) + \frac{|K_1'|}{12}. \tag{19}$$

When $K_1' > 0$ and the [001] easy axis is aligned with the rotational axis, the saddle points for magnetocrystalline anisotropy do not coincide with the hard axis for shape anisotropy. Nevertheless, the above expression is an upper bound for $\Delta g$, so it provides a lower bound on $L_{\rm SPM}$. The expression is exact for a sphere and approaches the correct $\Delta g$ asymptotically for $\mu_0 M_s^2 (N_x - N_z) \gg |K_1'|/6$. For the materials we consider in this paper, $L_{\rm SPM}$ changes little with elongation, so our expression is a good approximation to the exact $L_{\rm SPM}$.

No rigorous solutions for the energy critical size $L_0$ have been calculated, but there are upper and lower bounds. Clearly, $L_0 \le L_{\rm SD}^{\rm rem}$ in general, since the SD state is unstable for $L > L_{\rm SD}^{\rm rem}$. Of course, this upper bound is not useful if $L_{\rm SD}^{\rm rem}$ is infinite. In addition, for a prolate ellipsoid whose long axis is also a magnetocrystalline easy axis, *Aharoni* [1988] obtained the lower bound

$$L_0 \ge L_0^0 \equiv q^{1/3} L_{ex} \left(\frac{k}{N_z}\right)^{1/2}. \tag{20}$$

When $K_1 = \sigma = 0$, $L_{\rm SD}^{\rm rem}$ (17) reduces to the expression on the right, which is why we have called it $L_0^0$. Combining $L_0^0 = L_{\rm SD}^{\rm rem}$ with the upper bound, $L_0 = L_{\rm SD}^{\rm rem}$. Surprisingly, no one had previously noticed that the upper and lower bounds converge for a magnetically isotropic material.

When the internal (magnetocrystalline or magnetoelastic) easy axis does not coincide with the long axis, the lower bound on $L_0$ does not apply. The same is true for an oblate spheroid. The critical size $L_{\rm SD}^{\rm coerc}$, which is independent of internal anisotropy, is probably a lower bound for $L_0$.

**Table 1.** Magnetic Parameters Used to Calculate the Room Temperature Critical Sizes for Three Titanomagnetite Compositions

| Parameter | Magnetite | TM10 | TM60 |
|---|---|---|---|
| $M_s$(Am$^{-1}$) | $4.8 \times 10^5$ | $4.2 \times 10^5$ | $1.25 \times 10^5$ |
| $A$(Jm$^{-1}$) | $1.3 \times 10^{-11}$ | $1.0 \times 10^{-11}$ | $0.5 \times 10^{-11}$ |
| $K_1'$(Jm$^{-3}$) | $-1.1 \times 10^4$ | $-2.5 \times 10^4$ | $0.3 \times 10^4$ |
| $\lambda_{100}$ | $-19 \times 10^{-6}$ | – | $140 \times 10^{-6}$ |
| $\lambda_{111}$ | $78 \times 10^{-6}$ | – | $95 \times 10^{-6}$ |

The parameter $K_1'$ is the zero-strain magnetocrystalline anisotropy constant.

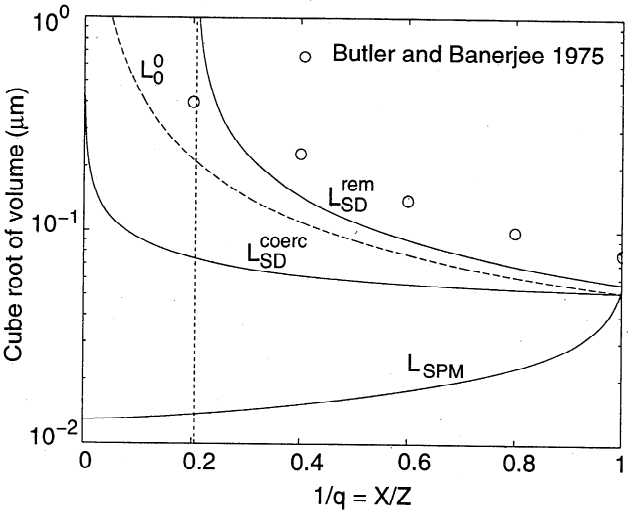


**Figure 3.** The critical sizes for magnetite are plotted as a function of inverse aspect ratio $1/q = X/Z$ in order to represent the full range of prolate spheroids. The vertical dashed line is the asymptote for $L_{\rm SD}^{\rm rem}$. The calculations of *Butler and Banerjee* [1975], converted to the cube root of the volume, are shown as open circles.

### 2.3. Critical Sizes for Titanomagnetites

In this section, we use (12)-(20) to calculate critical sizes for solid solutions of magnetite and ulvöspinel. We list the room temperature magnetic parameters in Table 1, and we discuss them in the appendix. For calculating $L_{\rm SPM}$, we use $\tau_s \approx \pi \times 10^7$ s (1 year). Changing $\tau_s$ to 100 s or 1 billion years changes $L_{\rm SPM}$ by only 15%. Following the discussion in section 2.2, we use $k = 20$.

**2.3.1. Theoretical predictions.** In Figure 3, we plot the critical sizes for magnetite. In calculating $L_{\rm SD}^{\rm rem}$, we assume the [111] easy axis is in the $z$ direction. We also plot the calculations of $L_0$ by *Butler and Banerjee* [1975] for comparison.

For a sphere of magnetite, The size range for SD remanence is very narrow ($L_{\rm SD}^{\rm rem} = 1.07 L_{\rm SD}^{\rm coerc}$). In addition, $L_{\rm SPM} > L_{\rm SD}^{\rm coerc}$, so there is no size at which ideal SD hysteresis occurs. However, the uncertainty in the exchange constant $A$ is enough (see the ppendix) that we cannot rule out larger ranges for SD remanence and coercivity. As the aspect ratio $q = Z/X$ increases, $L_{\rm SPM}$ decreases rapidly at first and then levels off. Our $L_{\rm SPM}$ curve looks different from previously published curves because previous authors defined the grain size as the long or short side.

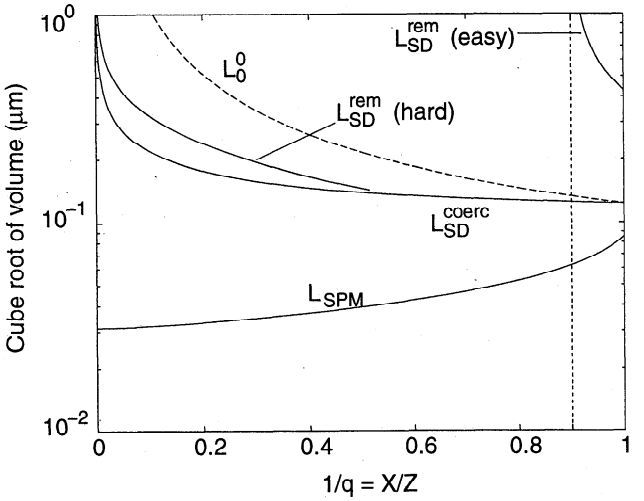


**Figure 4.** Critical sizes for TM60 (same conventions as in Figure 3). The vertical dashed line is the asymptote for $L_{SD}^{rem}$. The critical size $L_{SD}^{rem}$ is plotted for two extreme cases: alignment of the long axis with the easy and hard axes. In the latter case, $L_{SD}^{rem}$ is meaningful only for $L_{SD}^{rem} > L_{SD}^{coerc}$, so we stop the curve just before it crosses $L_{SD}^{coerc}$.

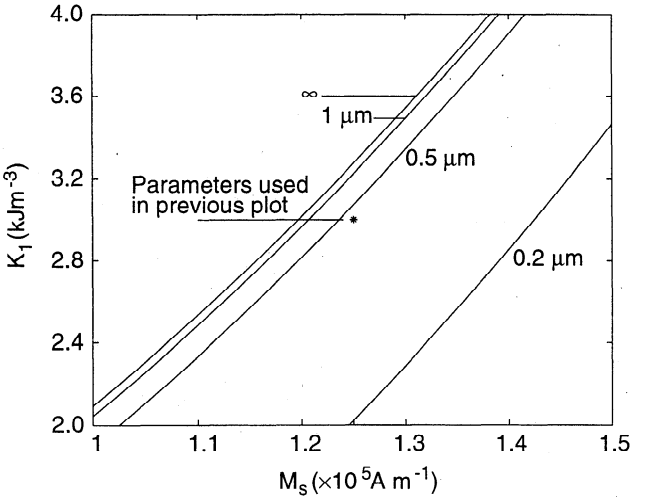


**Figure 5.** Contours of the SD remanence critical size $L_{SD}^{rem}$ as a function of possible values of $K_1$ and $M_s$ for TM60. The combination of parameters we used in Figure 4 is represented by an asterisk. A 10% change in $K_1$ or $M_s$ can make $L_{SD}^{rem}$ infinite.

The SD coercivity critical size $L_{SD}^{coerc}$ is weakly dependent on elongation except for $q \gtrsim 10$. By contrast, $L_{SD}^{rem}$ approaches infinity as the aspect ratio approaches 5. The asymptote for $L_{SD}^{rem}$ satisfies the equation $H_K + H_\lambda = M_s N_z$. Thus large, highly elongated grains of magnetite can have SD remanence, but this remanence will be less stable than the theory for uniform rotation predicts.

The above calculations are for zero stress. If a uniaxial tensile stress ($\sigma > 0$) is applied along the [111] axis, $L_{SD}^{coerc}$ is unaffected, but $L_{SD}^{rem}$ increases. However, for a sphere of magnetite, it takes a large stress to have much effect. Without stress, $L_{SD}^{rem} = 0.057\,\mu$m. To increase $L_{SD}^{rem}$ to $0.1\,\mu$m, a stress of 240 MPa is required.

In Figure 4, we plot the critical sizes for stress-free TM60 (60 mol % ulvöspinel). Comparing Figures 3 and 4, we see that the critical sizes $L_{SPM}$ and $L_{SD}^{coerc}$ are weakly dependent on composition, but $L_{SD}^{rem}$ can be very sensitive. We plot $L_{SD}^{rem}$ for the [001] easy axis in the $z$ direction and for the [111] hard axis in the $z$ direction. These curves show the importance of crystallographic orientation: When the hard axis is aligned with the long axis of the grain, the gap between $L_{SD}^{coerc}$ and $L_{SD}^{rem}$ almost disappears.

In Figure 4, the magnetic parameters we use for TM60 are our estimates of the mean values (appendix). In Figure 5, we show what happens if we vary these parameters. A change in $K_1'$ or $M_s$ of only 10% can increase $L_{SD}^{rem}$ from about $0.5\,\mu$m to infinity. A tensile stress of 1.3 MPa has the same effect.

Finally, in Figure 6, we plot the critical sizes for TM10 (10 mol % ulvöspinel). As titanium content increases from zero (magnetite), $K_1'$ initially remains negative but increases in magnitude while $M_s$ decreases [*O'Reilly*, 1984]. The critical sizes for a sphere do not change much, but the asymptote shifts from $q = 5$ to $q = 2.3$. We will discuss the significance of this shift in section 2.3.2.

**2.3.2. Comparison with domain observations.** The critical sizes can be compared most directly with domain observations. If a grain has developed a visible domain wall, it has certainly nucleated (the converse is not necessarily true). Thus nucleation theory can place bounds on domain wall formation. As we argue in section 3.1, the value of $L_{SD}^{rem}$ predicted by nucleation theory should be the upper limit for SD remanence in a real grain.

The value of $L_{SD}^{rem}$ for spherical, unstressed magnetite grains is only $0.057\,\mu$m. This limit is still near $0.1\,\mu$m

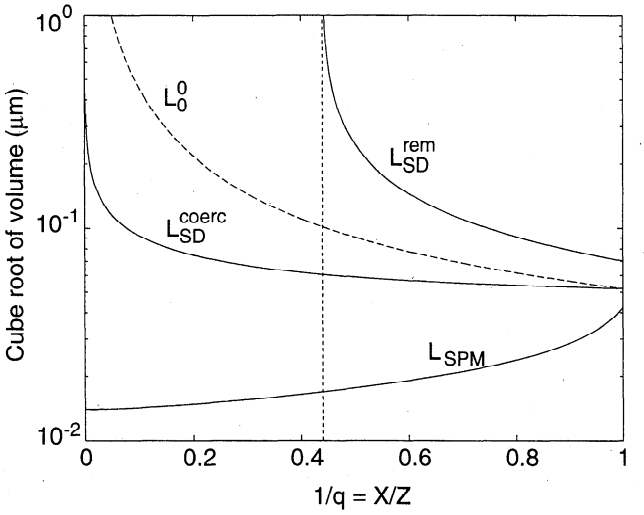


**Figure 6.** Critical sizes for TM10 (same conventions as in Figure 3). The asymptote for $L_{SD}^{rem}$ is shown as a vertical dashed line.

if the aspect ratio is increased to 2. This seems to contradict the observations of *Boyd et al.* [1984], who observed apparently SD states in two grains of natural magnetite that were $30 - 40\,\mu$m in size. The stability of these states varied when a reverse field was applied. Most developed domain walls in fields less than 10 mT, but one was stable in fields above 20 mT [*Boyd,* 1986]. No other investigators have found SD states in magnetite grains, even down to the present observational limit of about half a micron [*Smith,* 1980; *Geiß et al.,* 1996].

It is possible that the observations are misleading. Firstly, *Geiß et al.* [1996] examined only 10 magnetite grains, while *Boyd* [1986] examined a much larger number, so SD remanent states may turn up if more of the micron-size magnetite grains are examined. However, the SD state should be much more common in the grains that *Geiß et al.* [1996] observed because they are smaller. Secondly, as *Geiß et al.* [1996] acknowledged, they did not use a large enough field to ensure complete removal of preexisting domains. Thus their grains may not have started out saturated. Finally, the remanent states observed by *Boyd et al.* [1984] may have had nonuniform magnetization that was not imaged by the Bitter pattern technique.

If the observations of *Boyd et al.* [1984] are taken at face value, they could indicate a large uniform stress (hundreds of megapascals), although it is not clear what the origin of such a stress would be. Another possibility is that their magnetites are impure. As our calculations in section 2.3.1 showed, if only 10% ulvöspinel is added, $L_{\mathrm{SD}}^{\mathrm{rem}}$ is infinite for grains with elongations greater than 2.3. The grains observed by *Boyd et al.* [1984] have comparable elongations.

In observations of saturation remanence in TM60 grains, *Halgedahl and Fuller* [1980, 1983] saw both SD and MD states over a wide range of grain sizes. If TM60 is stress-free, it has a cubic anisotropy (with $K_1 > 0$), and $L_{\mathrm{SD}}^{\mathrm{rem}}$ is highly sensitive to small changes in composition, shape or crystallographic orientation. In practice, domain observations of TM60 suggest that the anisotropy is usually dominated by stress and is uniaxial. Depending on the orientation of the stress-induced easy axes, this may increase or decrease the size range for SD remanence. *Halgedahl and Fuller* [1980, 1983] claimed that the nonuniform states occurred because defects promote nucleation, but easy axis orientation is another possible mechanism.

Where $L_{\mathrm{SD}}^{\mathrm{rem}} \gg L_{\mathrm{SD}}^{\mathrm{coerc}}$, the coercivity will decrease considerably before the remanence starts to decrease. *Levi and Merrill* [1978] found that some highly elongated ($q \approx 8$) grains of magnetite had values of $M_{rs}$ around $0.45M_s$, close to the theoretical value ($0.5M_s$) for randomly oriented SD grains. The coercivity for randomly oriented, highly elongated SD grains ($N_x - N_z \approx 1$) should be $0.5M_s$ if they reverse by uniform rotation, but the observed coercivities were one sixth that value.

## 3. Discussion

Nucleation theory remains an esoteric and frequently misunderstood subject even among micromagnetic theorists. In part, this is because the theory determines only whether the SD state is stable; it does not say what happens after it becomes unstable and how this relates to observations. In sections 3.1 and 3.2, we discuss the form nucleation takes in small and large grains and the relationship of nucleation to hysteresis.

### 3.1. Nucleation in Small and Large Grains

In SD grains with uniaxial anisotropy [*Stoner and Wohlfarth,* 1947], there are at most two stable states at any given field. If one of these states becomes unstable, the magnetization must jump to the other state. The field at which the jump occurs was aptly named the switching field by *Schabes and Bertram* [1988]. The switching field is the single-grain analogue of the coercivity of remanence.

Most theorists assume that when nucleation occurs there must be a jump from one state to another, yet in a numerical model for a sphere [*Aharoni and Jakubovics,* 1990], the magnetization decreases continuously from saturation. The jump between states in the Stoner-Wohlfarth model occurs because one of the energy minima disappears, but this is not the only kind of instability. At another kind, a pitchfork bifurcation, a single minimum splits in two. As a state moves toward a bifurcation, it evolves along a single path until it reaches a fork at the bifurcation; it must then choose which path to take. Both new paths evolve continuously out of the old.

*Newell and Merrill* [1998] show that nucleation by the curling mode is a bifurcation. The mode $\mathbf{u}$ described by (1), and its opposite $-\mathbf{u}$, have the same effect on the energy. There is no reason to choose one over the other. After nucleation occurs, the SD state evolves continuously into a curling (vortex) state. At the nucleation field, there is a sudden change in the slope of the magnetization curve [*Aharoni and Jakubovics,* 1990; *Newell and Merrill,* 1998].

Thus the nucleation field must be distinguished from the switching field. Since the magnetization changes continuously at the nucleation field, it is not associated with obvious changes in the domain structure such as the appearance of domain walls. However, nucleation must occur before a domain wall appears.

For most of our calculations, the magnetocrystalline easy axis was parallel to the long axis. This is the most favorable orientation for maintaining the SD state. If the easy axis is rotated, $L_{\mathrm{SD}}^{\mathrm{rem}}$ will decrease. In many natural samples there is probably no correlation between the easy axis and the long axis. We cannot determine the nucleation field for all orientations of the easy axis, but we can calculate it for the least favorable: alignment of the hard axis with the long axis. When we

did this for a grain of TM60, we found the gap between $L_{SD}^{coerc}$ and $L_{SD}^{rem}$ almost disappeared (Figure 4).

It has long been known that nucleation in real materials occurs much more easily than nucleation theory predicts. This is known as Brown's paradox. The deviation from theory is usually attributed to defects, although the role that defects play may depend on the size of the anisotropy (for a thorough discussion see *Aharoni* [1996]). In "hard" materials ($K_1/\mu_0 M_s^2 \gg 1$), defects probably create centers for nucleation by lowering the local anisotropy. However, the same defects that allow nucleation centers to appear may also prevent them from spreading, so their effect on hysteresis properties is not obvious. In "soft" materials ($K_1/\mu_0 M_s^2 \ll 1$), such as magnetite, the most likely nucleation centers are surface imperfections that affect the local demagnetizing field.

The ellipsoid is the only known shape for which the demagnetizing field is uniform. As a result, the two nucleation modes (uniform rotation and curling) are exactly the same at all grain sizes. Despite the name "nucleation," which implies that the mode is concentrated in a small region, the nucleation modes are nonlocal.

In nonellipsoidal grains, the magnetization is never uniform. In the cube, the SD state (also called the flower state [*Schabes and Bertram,* 1988]) has a small divergence in the magnetization near the surface. If the magnetization were uniform, the demagnetizing field would be infinite in the corners. *Shtrikman and Treves* [1960] predicted this would make nucleation easier and concentrate it in the corners. However, the divergent magnetization in the flower state screens the field in the corners. *Newell and Merrill* [1998] show that as the size of a cubic grain increases, the nucleation mode changes gradually from a global curling mode like that in the sphere to a local mode. Nucleation is indeed easier in the cube, but the mode is concentrated in the centers of two opposing faces rather than the corners. The nucleation field fits a modified version of (8) quite well near $L_{SD}^{coerc}$, but as the size increases the nucleation field increases more rapidly than (8) predicts.

In summary, our calculations of the critical sizes are for ideal, highly symmetric grains. However, there are good theoretical and experimental reasons to assume that (16) is a good approximation to $L_{SD}^{coerc}$ in real grains, while (17) is an upper limit for the actual $L_{SD}^{rem}$.

The size range for SD remanence will be greatest for saturation remanence and smaller for other kinds of remanence. Strictly speaking, the nucleation calculations are for saturation remanence, since they assume there is initially a large field. There may be other states below $L_{SD}^{rem}$, such as curling states with moments perpendicular to the long axis [*Enkin and Williams,* 1994; *Newell,* 1997]. These states may dominate thermoremanent magnetization (TRM) and anhysteretic remanent magnetization (ARM) while the saturation remanence is still SD.

### 3.2. Nucleation and Hysteresis

We have described the relationship between nucleation and domain wall formation. What about hysteresis parameters? As we discussed above, nucleation always precedes switching (the transition from positive to negative remanence in a single grain). In principle, the nucleation field could be used as a bound on the coercivity of remanence. However, this is useful only when $H_n^{curl}$ is negative ($L < L_{SD}^{rem}$).

The critical sizes are more easily related to changes in the hysteresis parameters with grain size. The smallest grains are superparamagnetic and have no coercivity or remanence. As the size increases above $L_{SPM}$, both $H_c$ and $M_{rs}$ increase initially because thermal fluctuations decrease in importance. When the size exceeds $L_{SD}^{coerc}$, nucleation occurs by nonuniform rotation and $H_c$ decreases. Thus $H_c$ is a maximum at the grain size $L_{SD}^{coerc}$. The remanence continues to increase until $L = L_{SD}^{rem}$, at which point the SD state becomes unstable. Thus $M_{rs}/M_s$ is a maximum at $L_{SD}^{rem}$.

In trying to fit the grain size dependence of hysteresis parameters to theory, previous authors have assumed the grains in a sample can be represented by grains of a single size, the mean size [e.g., *Williams and Dunlop,* 1989]. However, the grains typically span an order of magnitude in size. Most of the synthetic samples are nearly spherical, and we predict the SD size range for equant grains will be small to nonexistent. This is probably the reason why many synthetic samples that are nominally in the SD size range have values of $M_{rs}/M_s$ that are well below 0.5, the value predicted by Stoner-Wohlfarth theory. Much of the non-SD behavior in these samples that is attributed to grain interactions [e.g., *Dunlop and Özdemir,* 1997] may be due to the size distribution.

While $L_{SD}^{rem}$ depends on composition as well as grain shape and other sources of anisotropy, $L_{SD}^{coerc}$ is much the same for titanomagnetites of all compositions and shapes. The size range between $L_{SPM}$ and $L_{SD}^{coerc}$ is always narrow. Thus, in real samples with a range of grain sizes, the coercivity will always be well below the SD value.

## 4. Conclusions

We had two main goals in this paper. The first was to make use of nucleation theory. The literature on nucleation is forbidding, but the solutions for the nucleation field are among the very few rigorous analytical solutions for nonuniform magnetization. In most fields, analytical solutions (even of very simple, idealized cases) are used as a starting point for numerical solutions. By contrast, nucleation theory has been neglected even by experts on micromagnetics. Yet some of the results obtained by nucleation theory are very simple. For example, in perfect spheroidal grains, there are only two possible nucleation modes, uniform rota-

tion and curling, when the applied field is parallel to the axes of anisotropy. The nucleation field for the curling mode has a $1/L^2$ dependence on grain size.

In this paper, we have presented the theory for perfect spheroidal grains. We have also shown how this idealized theory is related to observations of imperfect, nonspheroidal grains. Recently, *Newell and Merrill* [1998] identified the nucleation mode in a cube, and showed that it evolves from a curling mode like that in a sphere to a more localized curling mode in larger grains. As the nucleation mode becomes more localized, nucleation becomes easier than the analytical theory predicts. When nucleation occurs, the magnetization changes continuously so there is no observable change in domain structure, but nucleation precedes domain wall formation.

Our second goal was to show that there is more than one critical size for SD properties. Previous authors [e.g., *Dunlop and Özdemir,* 1997] have noted that the usual energy-based critical size $L_0$ has an uncertain meaning. Now we have used nucleation theory to calculate the critical sizes $L_{SD}^{coerc}$ for coercivity and $L_{SD}^{rem}$ for remanence. The analytical form of our equations makes it easy to explore the effect of varying shape, composition, stress, or the orientation of easy axes; by modifying the equations for cubic anisotropy with $K_1 < 0$, we can apply them to titanomagnetites.

We find that the coercivity critical size $L_{SD}^{coerc}$ varies little with composition or shape in the titanomagnetite series and is not affected by stress or magnetocrystalline anisotropy. By contrast, the remanence critical size $L_{SD}^{rem}$ varies greatly. For nearly equant magnetite grains, the size range for SD remanence is small to nonexistent. This probably explains why synthetic samples with mean sizes that are nominally SD have properties that do not agree well with the predictions of Stoner-Wohlfarth or Néel theory.

As numerical micromagnetic calculations become easier, they will replace existing domain theories. It is important to anchor the numerical work with analytical results. If possible, the nucleation field should be calculated for arbitrary orientations of the field, and the relationship between the nucleation field and the switching field should be explored. We should also try to determine what critical sizes apply to reliable Thellier-Thellier tests, the Lowrie-Fuller test, and other tests of importance to paleomagnetism.

## Appendix: Magnetic Parameters for Titanomagnetites

The magnetic parameters listed in Table 1 are reasonably well known for magnetite, but in the rest of the series $Fe_{3-x}Ti_xO_4, 0 \leq x \leq 1$, there is considerable uncertainty because the parameters are sensitive to differences in stoichiometry [*O'Reilly,* 1984]. Indeed, the exact composition of a titanomagnetite is often uncertain because there is inconsistency between different methods of determining the level of oxidation, there are uncertainties in cation ordering, and there tend to be small-scale chemical inhomogeneities [*Moskowitz,* 1987]. Often, theorists are tempted to understate the uncertainty because it is too laborious to repeat numerical calculations with different parameters, but with the simple expressions that we have developed in this paper, it is easy to assess the effect on the critical sizes of changing parameters.

Below we review the measurements of each parameter at room temperature for magnetite and TM60 ($Fe_{2.4}Ti_{0.6}O_4$).

### A1. Saturation Magnetization

For magnetite, $M_s$ is $4.8 \times 10^5\,Am^{-1}$. For TM60, the range of experimental estimates is $(1 - 1.5) \times 10^5\,Am^{-1}$ [*O'Reilly,* 1984].

### A2. Exchange Constant

In principle, $A$ can be determined from inelastic neutron scattering and other methods, but for ferrimagnets the interpretation of the measurements is complex and the values of $A$ do not always agree well. *Moskowitz and Halgedahl* [1987] and *Heider and Williams* [1988] reviewed existing measurements and obtained an average of $A = 1.3 \times 10^{-11}\,Jm^{-1}$. *Butler and Banerjee* [1975] used $A = 1.5 \times 10^{-11}\,Jm^{-1}$. *Moskowitz and Halgedahl* [1987] point out that because of uncertainties in two of the coupling constants, the uncertainty in $A$ could still be 50%.

For titanomagnetites other than magnetite, $A$ is estimated indirectly using assumptions about its dependence on composition and temperature [*Moskowitz and Halgedahl,* 1987]. It is probably reasonable to assume a range $A = (10^{-12} - 10^{-11})\,Jm^{-1}$. Fortunately, $A$ appears inside a square root in the expressions for the critical sizes, so this range corresponds to a change in the critical sizes of a factor of three. In Figure 4, we used $A = 5 \times 10^{-12}\,Jm^{-1}$.

### A3. Magnetocrystalline Anisotropy

As we mentioned in section 2.1, the constant that is actually measured is $K_1'$, the "zero-stress" constant. For magnetite, $K_1' = -1.1 \times 10^4\,Jm^{-3}$. As titanium content increases, $K_1'$ first decreases, then increases to positive values [*O'Reilly,* 1984]. *Moskowitz and Halgedahl* [1987] estimate $K_1' = 0.4 \times 10^4\,Jm^{-3}$ for TM60 by interpolating the measurements of *Syono* [1965]. For TM61, *Sahu and Moskowitz* [1995] measure $K_1' = 0.2 \times 10^4\,Jm^{-3}$. Since the compositions of TM60 and TM61 are so close, these measurements indicate the uncertainty in $K_1'$ for TM60.

### A4. Magnetostriction

For magnetite, $\lambda_{100}$ is $-19 \times 10^{-6}$, and $\lambda_{111}$ is $78 \times 10^{-6}$ [*Fletcher and O'Reilly,* 1974]. For TM60, we use the measurements by *Sahu and Moskowitz* [1995] for TM61: $\lambda_{100} = 140 \times 10^{-6}$ and $\lambda_{111} = 95 \times 10^{-6}$.

**Acknowledgments.** The authors thank the Earth Science division of NSF for supporting this research. Reviews by Rainer Heller, Susan Halgedahl, Michel Prévot, and an anonymous referee led to substantial improvements in the manuscript.

## References

Aharoni, A., Some recent developments in micromagnetics at the Weizmann Institute of Science, *J. Appl. Phys., 30*, 70S–78S, 1959.

Aharoni, A., Magnetization curling, *Phys. Status Solidi, 16*, 1–42, 1966.

Aharoni, A., Elongated single-domain ferromagnetic particles, *J. Appl. Phys., 63*, 5879–5882, 1988.

Aharoni, A., *Introduction to the Theory of Ferromagnetism*, 315 pp., Oxford Univ. Press, New York, 1996.

Aharoni, A., Nucleation modes in ferromagnetic prolate spheroids, *J. Phys. Condens. Matter, 9*, 10,009–10,021, 1997.

Aharoni, A., and J. P. Jakubovics, Approach to saturation in small isotropic spheres, *J. Magn. Magn. Mater., 83*, 451–452, 1990.

Aharoni, A., and S. Shtrikman, Magnetization curve of the infinite cylinder, *Phys. Rev., 109*, 1522–1528, 1958.

Boyd, J. R., Domain observations on naturally occurring magnetite, M.A. thesis, 169 pp., Univ. of Calif. Santa Barbara, Aug. 1986.

Boyd, J. R., M. Fuller, and S. Halgedahl, Domain wall nucleation as a controlling factor in the behaviour of fine magnetic particles in rocks, *Geophys. Res. Lett., 11*, 193–196, 1984.

Brown, W. F. Jr., *Micromagnetics*, 143 pp., Interscience, New York, 1963. (Reprinted by Krieger, New York, 1978.)

Butler, R. F., and S. K. Banerjee, Theoretical single–domain grain size range in magnetite and titanomagnetite, *J. Geophys. Res., 80*, 4049–4058, 1975.

Chikazumi, S., *Physics of Magnetism*, 554 pp., John Wiley, New York, 1964.

Dunlop, D. J., and Ö. Özdemir, *Rock Magnetism: Fundamentals and Frontiers*, 573 pp., Cambridge Univ. Press, New York, 1997.

Enkin, R. J., and D. J. Dunlop, A micromagnetic study of pseudo single-domain remanence in magnetite, *J. Geophys. Res., 92*, 12,726–12,740, 1987.

Enkin, R. J., and W. Williams, Three-dimensional micromagnetic analysis of stability in fine magnetic grains, *J. Geophys. Res., 99*, 611–618, 1994.

Evans, M. E., and M. W. McElhinny, An investigation of the origin of stable remanence in magnetite-bearing rocks, *J. Geomagn. Geoelectr., 4*, 142–146, 1969.

Fabian, K., A. Kirchner, W. Williams, F. Heider, A. Hubert, and T. Leibl, Three-dimensional micromagnetic calculations for magnetite using FFT, *Geophys. J. Int., 124*, 89–104, 1996.

Fletcher, E. J., and W. O'Reilly, Contribution of $Fe^{2+}$ ions to the magnetocrystalline anisotropy constant $K_1$ of $Fe_{3-x}Ti_xO_4, 0 \leq x \leq 0.55$, *J. Phys. C Solid State Phys., 7*, 171–178, 1974.

Geiß, C. E., F. Heider, and H. C. Soffel, Magnetic domain observations on magnetite and titanomaghemite grains ($0.5 - 1.0\,\mu$m), *Geophys. J. Int., 124*, 75–88, 1996.

Halgedahl, S., and M. Fuller, Magnetic domain observations of nucleation processes in fine particles of intermediate titanomagnetite, *Nature, 288*, 70–72, 1980.

Halgedahl, S., and M. Fuller, The dependence of magnetic domain structure upon magnetization state with emphasis upon nucleation as a mechanism for pseudo-single-domain behavior, *J. Geophys. Res., 88*, 6505–6522, 1983.

Heider, F., and W. Williams, Note on temperature dependence of exchange constant in magnetite, *Geophys. Res. Lett., 15*, 184–187, 1988.

Kirschvink, J. L., and H. A. Lowenstam, Mineralization and magnetization of chiton teeth: palcomagnetic, sedimentologic, and biologic implications of organic magnetite, *Earth Planet. Sci. Lett., 44*, 193–204, 1979.

Kittel, C., Theory of the structure of ferromagnetic domains in films and small particles, *Phys. Rev., 70*, 965–971, 1946.

Kittel, C., Physical theory of ferromagnetic domains, *Rev. Mod. Phys., 21*, 541–583, 1949.

Landau, L., and E. Lifshitz, On the theory of the dispersion of magnetic permeability in ferromagnetic bodies, Phys. Z. Sowjetunion, 8, 153-169, 1935. (Reprinted in *Collected Papers of L. D. Landau*, edited by D. ter Haar, pp. 101–114, Pergamon, Tarrytown, N.Y., 1965.)

Levi, S., and R. T. Merrill, Properties of single-domain, pseudo-single-domain, and multidomain magnetite, *J. Geophys. Res., 83*, 309–323, 1978.

Moon, T., and R. T. Merrill, The magnetic moments of nonuniformly magnetized grains, *Phys. Earth Planet. Inter., 34*, 186–194, 1984.

Morrish, A. H., and S. P. Yu, Dependence of the coercive force on the density of some iron oxide powders, *J. Appl. Phys., 26*, 1049–1055, 1955.

Moskowitz, B. M., Towards resolving the inconsistencies in characteristic physical properties of synthetic titanomaghemites, *Phys. Earth Planet. Inter., 46*, 173–183, 1987.

Moskowitz, B. M., and S. L. Halgedahl, Theoretical temperature and grain-size dependence of domain state in $x = 0.6$ titanomagnetite, *J. Geophys. Res., 92*, 10,667–10,682, 1987.

Nagata, T., *Rock Magnetism*, rev. ed., 350 pp., Maruzen, Tokyo, 1961.

Néel, L., Propriétés d'un ferromagnétique cubique en grains fins, *C. R. Acad. Sci. Paris, 224*, 1488–1490, 1947.

Néel, L., Théorie du trainage magnétique des ferromagnétiques en grains fins avec application aux terres cuites, *Ann. Géophys., 5*, 99–136, 1949.

Newell, A. J., Theoretical Calculations of Magnetic Hysteresis and Critical Sizes For Transitions Between Single-domain and multi-domain Properties in Titanomagnetites, Ph.D. dissertation, 188 pp., Univ. of Wash., Seattle, Oct. 1997.

Newell, A. J., and R. T. Merrill, The curling nucleation mode in a ferromagnetic cube, *J. Appl. Phys., 84*, 4394-4402, 1998.

Newell, A. J., D. J. Dunlop, and R. J. Enkin, Temperature dependence of critical sizes, wall widths and moments in two-domain magnetite grains, *Phys. Earth Planet. Inter., 65*, 165–176, 1990.

Newell, A. J., D. J. Dunlop, and W. Williams, A two-dimensional micromagnetic model of magnetizations and fields in magnetite, *J. Geophys. Res., 98*, 9533–9550, 1993.

Opdyke, N. D., and J. E. T. Channell, *Magnetic Stratigraphy*, 346 pp., Academic, San Diego, Calif., 1996.

O'Reilly, W., *Rock and Mineral Magnetism*, 220 pp., Blackie, New York, 1984.

Ricci, J. C. D., and J. L. Kirschvink, Magnetic domain state and coercivity predictions for biogenic greigite ($Fe_4S_4$): A comparison of theory with magnetosome observations, *J. Geophys. Res., 97*, 17,309–17,316, 1992.

Sahu, S., and B. M. Moskowitz, Thermal dependence of magnetocrystalline anisotropy and magnetostriction constants of single crystal $Fe_{2.4}Ti_{0.61}O_4$, *Geophys. Res. Lett., 22*, 449–452, 1995.

Schabes, M. E., and H. N. Bertram, Magnetization processes in ferromagnetic cubes, *J. Appl. Phys., 64*, 1347–1357, 1988.

Shtrikman, S., and D. Treves, On the resolution of Brown's paradox, *J. Appl. Phys., 31*, 72S-73S, 1960.

Smith, P. P. K., The application of Lorentz electron microscopy to the study of rock magnetism, in *Electron Microscopy and Analysis, 1979*, edited by T. Mulvey, pp. 125-128, Inst. of Phys., Bristol, England, 1980.

Stacey, F. D., The physical theory of rock magnetism, *Adv. Phys., 12*, 45–133, 1963.

Stoner, E. C., and E. P. Wohlfarth, A mechanism of magnetic hysteresis in heterogeneous alloys, *Philos. Trans. R. Soc. London, Ser. A, 240*, 599–642, 1947.

Syono, Y., Magnetocrystalline anisotropy and magnetostriction of $Fe_3O_4 - Fe_2TiO_4$ series - with special application to rock magnetism, *Jpn. J. Geophys., 4*, 71–143, 1965.

Thompson, R., and F. Oldfield, *Environmental Magnetism*, 227 pp., Allen and Unwin, Winchester, Mass., 1986.

Williams, W., and D. J. Dunlop, Three-dimensional micromagnetic modelling of ferromagnetic domain structure, *Nature, 337*, 634–637, 1989.

Ye, J., A. J. Newell, and R. T. Merrill, A re-evaluation of magnetocrystalline anisotropy and magnetostriction constants, *Geophys. Res. Lett., 21*, 25–28, 1994.

R. T. Merrill and A. J. Newell, Geophysics Program, Box 351650, University of Washington, Seattle, WA 98195-1650. (e-mail: newell@geophys.washington.edu)

(Received February 26, 1998; revised August 26, 1998; accepted September 23, 1998.)